Flapping and Bending Bodies Interacting with Fluid Flows

Michael J. Shelley and Jun Zhang

Applied Mathematics Lab, Courant Institute of Mathematical Sciences, New York University, New York, New York 10012; email: shelley@cims.nyu.edu, jun@cims.nyu.edu

Annu. Rev. Fluid Mech. 2011. 43:449–65

First published online as a Review in Advance on September 22, 2010

The *Annual Review of Fluid Mechanics* is online at fluid.annualreviews.org

This article's doi: 10.1146/annurev-fluid-121108-145456

0066-4189/11/0115-0449$20.00

Keywords

fluid-body interactions, flags, flutter, flexible bodies, instability, drag reduction, flapping

Abstract

The flapping or bending of a flexible planar structure in a surrounding fluid flow, which includes the flapping of flags and the self-streamlining of flexible bodies, constitutes a central problem in the field of fluid-body interactions. Here we review recent, highly detailed experiments that reveal new nonlinear phenomena in these systems, as well as advances in theoretical understanding, resulting in large part from the rapid development of new simulation methods that fully capture the mutual coupling of fluids and flexible solids.

1. BACKGROUND

An archetype of fluid-structure interactions is the flapping of a flag in a steady wind, and the mutual motion of wind and fabric has long begged the question of the causal factors. For example, **Figure 1** depicts the well-known and possibly apocryphal story that relates the contribution of the Chinese Buddhist master Hui-Neng (638–713) to an argument between two monks as they watched a temple flag flutter in the breeze. Listening as they argued back and forth, with one claiming "The flag flaps!" and the other replying "No, it is the wind that moves!", Hui-Neng interrupted the argument to tell them that they were both wrong, and that instead "It is the mind that moves." Although this might be so, it also diverted the framing of a fascinating scientific question that might be posed as whether the motions of the flag passively reflect the unseen dynamics of the fluid, or whether flag and wind are a coupled system with their motions jointly determined.

The flapping of flags is a subset of a more general class of fluid-structure problems that concern the interaction of flexible sheets or bodies with high-speed fluid flows. Sails are a classical example, whereas understanding the flapping of flexible sheets is important to applications such as paper processing (Watanabe et al. 2002), as well as to possible approaches to energy harvesting (Allen & Smits 2001) and turbulence reduction (Shen et al. 2003). In the natural world, biological structures are found to bend, fold, twist, and wave in air and water flows, with these responses often allowing the organism to survive its wavey or windy environment (Vogel 1994). Both the driven and intrinsic flapping of flexible structures are important to understanding the swimming of fish (Huber 2000, Liao et al. 2003, Muller 2003).

Over the past decade there has been considerable research into the basic dynamics of flexible structures that separate high-speed flows, with some of that work coming out of our laboratory at New York University. Thus, this review selectively covers recent experimental, theoretical, and numerical work related to the flapping and bending of flexible sheets in high-speed flows, as well as discusses some interesting extensions. Not reviewed here is a related set of important

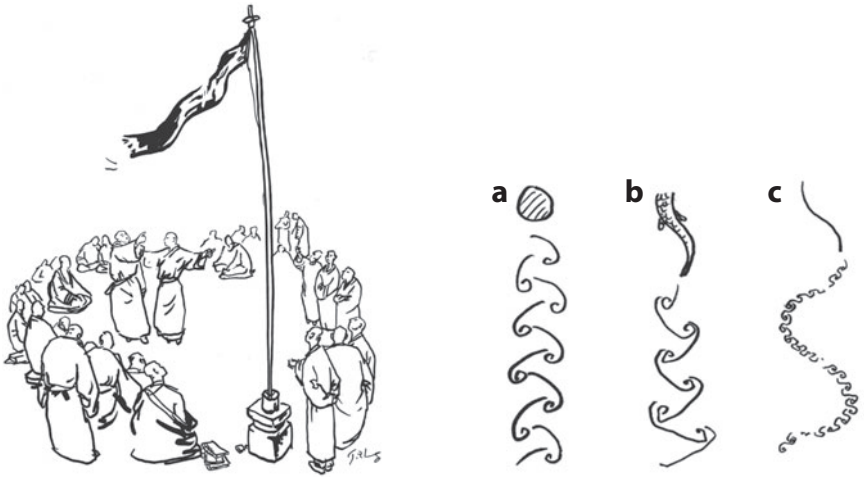

Figure 1

(*Left panel*) An artistic rendering of the story of Hui-Neng and the two monks. (*Right panel*) The structure of vortical wakes shed behind various types of bodies: (*a*) a rigid cylinder, showing the classical von Kármán vortex street associated with drag; (*b*) the thrust wake associated with the swimming of fish; and (*c*) that behind a flapping flag, showing both large- and small-scale vortical structures. Renderings courtesy of J. Zhang.

fluid-structure problems concerning the dynamics of flexible structures such as tubes in fluid flows (see de Langre et al. 2007, Paidoussis 2004, and references therein). Another rich area concerns the dynamics of flexible objects in low–Reynolds number flows, which is important to understanding microorganismal locomotion and complex fluids.

2. FLAPPING OF FLEXIBLE SHEETS IN FLOWS

As a theoretical problem, the phenomenon of flag flapping seems to have been addressed first by Rayleigh (1879), who, in studying the instability of jets, considered the dynamics of a two-dimensional (2D) vortex sheet [or surface of discontinuity (Saffman & Baker 1979)], of zero mean circulation, evolving in a 2D inviscid fluid. The displacement of such a vortex sheet from being flat, regardless of scale, shows a weak linear-in-time growth, and Rayleigh took this as being related to the "flapping of flags and sails." This model is perhaps most appropriate for describing the wake shed by a periodically flapping flag: Over one half-period, the vortex layer being shed is of positive sign, and over the other half it is negative, thus creating a vortex layer of zero mean circulation. One large missing piece in Rayleigh's model is a description of the inertial and internal mechanical forces of the flag. Beginning with the 1930s, such effects were studied by workers in aeroelasticity using a variety of approximate and empirical flow models (Bisplinghoff & Ashley 2002). To the present day, these approximate treatments have grown increasingly sophisticated and are well reviewed in the works of Eloy et al. (2007, 2008).

Over the past 10 years, new and detailed experiments have been performed, and numerical simulations have become increasingly accurate in their treatment of fluid-structure interactions. In the ensuing subsections, we first discuss several experimental studies of the interaction of flags with steady flows. This is followed by a review of simulational studies and recent reduced descriptive models.

2.1. Experimental Studies

The experimental study that appears to have first explored the flapping of flags in a uniform flow was performed in the mid-1960s by Taneda (1968). Taneda studied flags made of various fabrics (silk, muslin, flannel, canvas) and shapes (rectangles and triangles) hanging in a vertical wind tunnel, and his results anticipated many of the experimental and simulational studies of the past decade. He reported that flags in slow flows do not flap and are trailed by a thin von Kármán wake. The stability of this state may not be surprising given the jointly stabilizing effects of viscously and gravitationally induced tension in the fabric. However, increasing the flow speed induced regular oscillations in the flag, with a broad and wavey trailing vortex wake. Yet higher speeds led to irregular flapping. He reported a variety of observed flag-flapping modes—nodeless (apparently a traveling wave of deformation), one-node, imperfect-node, and two-node flutter—and reported bistability in which a flapping flag can be induced (by giving a "slight shock" to the flag) to move back and forth between 2D and 3D flapping states with different flapping frequencies. Taneda also reported substantially higher drag on the flag due to flapping.

It is unclear from Taneda's description the degree of uniformity of the imposed flow, and hence the contribution of external fluctuations to the observed dynamics. He also concluded that flag mass had little effect on the onset of flapping, which is not in accord with our current understanding, as is the statement that the inclusion of a downstream splitter plate showed little effect.

Taneda's work seems to have been the sole systematic study in this field up until our own lab revisited the problem in the simplified setting of soap-film flows (Zhang et al. 2000). As is

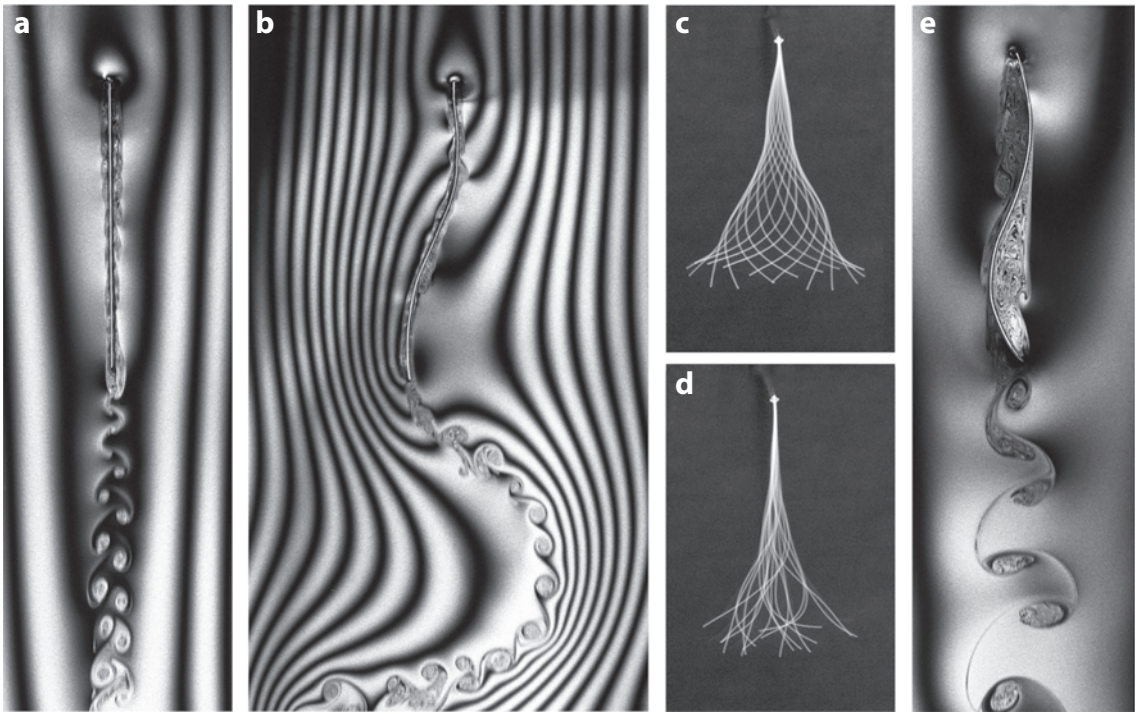

Figure 2

(*a*,*b*) Flow visualization of the wake structure downstream of a flexible filament made of silk thread and immersed in a running soap film. The light-dark bands are interference fringes created by reflection of a monochromatic light source. (*a*) The stretched-straight state. (*b*) Flapping. (*c*) A coherently flapping filament at several time points along its flapping cycle. (*d*) The same filament at higher flow speed, showing aperiodic flapping. (*e*) The flow around a stiff metal wire bent permanently into the shape of a flapping filament.

now well appreciated, a flowing soap film provides a reasonable facsimile of a 2D Navier-Stokes fluid (Rutgers et al. 2001) and has been used extensively to study a variety of flow phenomena (see Couder et al. 1989 and Gharib & Derango 1989 for two seminal studies). Our experiment takes place in a gravity-driven soap-film tunnel with a width of 10–15 cm and with downward flow speeds that lie in the range of 0.5–3 m s^{-1}. Into the plane of this film is inserted a length of silk thread, which is held at its upstream end but is otherwise free to move within the flow. This system constitutes what is essentially a 1D flag moving in a 2D wind. The flow is visualized using the interference fringes set up by reflection, from the front and back surfaces of the film, of monochromatic illumination. Planar Reynolds numbers are of order 10^4.

In this relatively simple setup, we have observed three distinct dynamical states. **Figure 2*a*** shows the so-called stretched-straight (SS) state in which the filament is unmoving and aligned with the flow. We note the narrow and well-defined von Kármán wake downstream of the flag's trailing end. **Figures 2*b*,*c*** show the filament moving in a coherent flapping mode, made up of sinuous traveling waves moving and amplifying downstream from the leading edge. The flow visualization strongly suggests that as in the SS state, the flapping filament sheds vorticity into the flow primarily from its trailing end, giving little indication of boundary-layer separation along the flexible body. Unlike the alternating-sign vortex structure in the wake of the SS case, the fine-scale vortices are now primarily of a single sign and correspond to the Kelvin-Helmholtz instability of a thin vortex layer being shed from the trailing end, with the overall sign of the shed layers

alternating with each half-stroke of the tail. Overall, the wake has a peculiar structure with some resemblance to a von Kármán drag wake that directs fluid momentum toward the body (see the various wake structures shown in **Figure 1**).

As a counterpoint, **Figure 2*e*** shows flow around a flag-like rigid body, made from wire and of the same scale and shape as that in **Figure 2*b***. Now that the deformation wave is not moving downward with the flow, it obstructs the flow, and boundary-layer separation leads to persistent vortices along the body, a very different boundary-layer structure, and a fluid drag that is two to three times larger than that measured in time average for the flexible filament (J. Zhang, unpublished data).

One very different aspect of these results from those of Taneda is that the bistability of the SS and flapping states (**Figures 2*a*,*b***) is of the same filament at the same flow speed. An associated hysteresis is revealed by using the filament length as a control parameter: At small filament length, the sole stable state appears to be the SS state. Slowly increasing the length, the SS state persists, but at a critical length L_1 its stability is lost and the system jumps to flapping (see Zhang et al. 2000, figure 3), where it remains as the length is further increased. If this is followed by a slow retraction of the length, the flapping dynamics persists well into the regime of the SS state, and then for some $0 < L_2 < L_1$, the system jumps back down to the SS state. Finally, the stroboscopic image in **Figure 2*d*** shows, as in Taneda (1968), the emergence of irregular flapping with an increase in filament length or flow speed (J. Zhang, unpublished data).

Fundamental aspects of this system are (*a*) loss of stability for the SS state to flapping and (*b*) bistability and hysteresis of the SS and flapping states. An experimental study by Watanabe et al. (2002) was motivated by paper flutter, a potentially destructive phenomenon in high-speed printing. They report instability, hysteresis, and bistability as a function of flow speed. Similarly, Shelley et al. (2005) observed these phenomena as a function of flow speed, for articulated metal flags flapping in a water tunnel. This latter study also highlighted the central importance of flag mass in system stability and understood the loss of stability of the SS state through a simple model system discussed below. Eloy et al. (2008) performed experiments in a wind tunnel of the flutter of Mylar sheets and investigated the effect (also theoretically) of sheet aspect ratio (span to length). Like other studies, they found a critical velocity at which the stability of the SS state was lost.

2.2. Theoretical Studies

Perhaps driven by these recent experiments, the past decade has seen many new theoretical treatments of fluid-flag interactions, especially in the development of simulation methods that fully couple the dynamics of flag and fluid. Indeed, simulating flag instability and flapping, and demonstrating bistability of SS and flapping states, has become a benchmark problem in this field. Thus far, most of these studies have been confined to two dimensions. In this section we selectively review theoretical work, focusing on a few key studies. We begin by describing recent work that instantiates a fully nonlinear version of Rayleigh's conception of a flag (or sail) as a surface of discontinuity in an inviscid fluid, where the flag and wake are treated in an integrated fashion. Although this work captures much of what is observed experimentally, it was actually preceded by simulations of the more complex Navier-Stokes equations, which are discussed below.

2.2.1. A nonlinear vortex sheet model. Let us consider a 2D inviscid and incompressible fluid of density ρ_f. Immersed in this fluid is an inextensible elastic sheet with coordinates $\mathbf{X}(s,t)$ (where s is the arc length), and of length L, rigidity E, and mass per unit length ρ_s (see the schematic of **Figure 4*a***). Its leading edge at $s = 0$ is fixed and clamped to align with an impinging uniform flow $U\,\hat{\mathbf{x}}$, while free-end boundary conditions are applied at $s = L$. Scaling space on L and time

on $T = L/U$, this system has only two nondimensional parameters:

$$R_1 = \frac{\rho_s}{\rho_f L} \quad \text{and} \quad R_2 = \frac{E}{\rho_f L^3 U^2}, \tag{1}$$

where R_1 is the dimensionless mass of the flag, and R_2 is its dimensionless rigidity (or inverse square velocity).

Were the fluid a viscous one, there would also be a Reynolds number defined as $Re = \rho_f UL/\mu$, with μ the fluid viscosity (plus an associated no-slip condition on the flag and more general stress jump across the flag). Instead, to model the effect of viscosity in producing vorticity within boundary layers along the flag, the flag is allowed to shed a vortex sheet from its trailing end. In particular, on the outer scale, we model the flag and its shed wake as a single vortex sheet (Saffman & Baker 1979) along a contour C and characterized by its sheet strength, $\gamma(s,t)$, that gives the size of the tangential velocity jump across C. We write $C = C_b + C_f$ (body plus fluid). The singular distribution of vorticity along C induces a velocity in the fluid through the Biot-Savart integral

$$\mathbf{u}(\mathbf{x}) = \hat{\mathbf{x}} + \frac{1}{2\pi}\int_C ds'\gamma(s')\frac{(\mathbf{x}-\mathbf{X}(s'))^\perp}{|\mathbf{x}-\mathbf{X}(s')|^2} \quad \text{with} \quad (x,y)^\perp = (-y,x). \tag{2}$$

Self-induction of the sheet is found through averaging the limits of $\mathbf{u}$ from above and below C, yielding

$$\mathbf{W}(s) = \hat{\mathbf{x}} + \frac{1}{2\pi}P\int_C ds'\gamma(s')\frac{(\mathbf{X}(s)-\mathbf{X}(s'))^\perp}{|\mathbf{X}(s)-\mathbf{X}(s')|^2}, \tag{3}$$

where the principal-value integral is the Birkhoff-Rott integral. Its normal component is the continuous normal part of $\mathbf{u}$ across C. The evolution equation for γ is found through differencing the Euler equations across C. Across C_f, where there is no pressure jump, it is most convenient to evolve γ in the average-velocity frame where γg, with g the arc-length metric, is invariant in time. On C_b, we find the forced advection equation

$$\gamma_t + (V\gamma)_s = -[p]_s, \tag{4}$$

where the scalar velocity V is that which keeps s independent of t (that is, the flag is inextensible). The two sheets C_b and C_f are coupled together at the flag's trailing end through an unsteady Kutta condition, arising from requirements of flow smoothness, which determines the rate of circulation flux from the bound sheet C_b into the free sheet C_f (see Jones 2003, Jones & Shelley 2005).

On the inner scale, the flag is considered an inextensible surface that moves through the balance of its own inertial forces, internal mechanical forces, with pressure forces from the surrounding fluid:

$$R_1\mathbf{X}_{tt} = (T\hat{\mathbf{n}})_s - R_2\mathbf{X}_{ssss} + [p]\hat{\mathbf{n}}. \tag{5}$$

Here the tension T is also the Lagrange multiplier that enforces material inextensibility.

2.2.2. A simple model system. The equations of motion are quite complicated, but to give their flavor, let us ignore all sorts of important and complicating factors and simply consider a bi-infinite and periodic flag linearized near a flat sheet. This gives a system for the vertical displacement η and sheet strength γ:

$$R_1\eta_{tt} = -R_2\eta_{xxxx} + [p], \tag{6}$$

$$\eta_t + \eta_x = \frac{1}{2}\mathcal{H}[\gamma], \quad \gamma_t + \gamma_x = -[p]_x, \tag{7}$$

where $\mathcal{H}[\cdot]$ is the nonlocal Hilbert transform (Carrier et al. 1966) that arises from linearizing the Birkhoff-Rott integral. We note that there is no tensile force term in Equation 6. In the absence

of viscous shear stresses or a gravitational body force aligned with the flag, tensile forces are determined only by the constraint of inextensibility. For linear perturbations from the flat state, this is a higher order effect. This is similar to the model used by Crighton & Oswell (1991) to study the interaction of an impinging potential flow with an infinite compliant wall.

This system is an interesting mix of nonadvective (Equation 6; the flag is held against the flow) and advective (Equation 7; the outer flow dynamics) equations and captures the nonlocal coupling of vorticity to velocity. It can be rewritten as the single scalar integro-differential equation

$$\eta_{tt} + 2\eta_{xt} + \eta_{xx} = -\frac{1}{2}\mathcal{H}[R_1\eta_{xtt} + R_2\eta_{xxxxx}], \tag{8}$$

and looking for solutions of the form $\eta = e^{i\omega t}e^{ikx}\hat{\eta}$ gives the quadratic dispersion relation

$$(\omega + k)^2 = \frac{1}{2}(-R_1|k|\omega^2 + R_2|k|^5).$$

The condition for instability (neutral stability) of a particular perturbation with wave number k is that the discriminant $d_k = R_1R_2|k|^3 + 2R_2|k|^2 - 2R_1$ is negative (positive).

There are several interesting aspects of this system. (*a*) At small length scales, the system is dispersively controlled by inertia and elasticity:

$$\omega \approx \pm\left(\frac{R_2}{R_1}\right)^{1/2} k^2 \quad \text{for} \quad k \gg 1.$$

(*b*) With no flag mass, $R_1 = 0$, the system is purely dispersive, showing no linear instability,

$$\omega = -k\left[1 \pm \left(\frac{R_2}{2}\right)^{1/2}|k|^{3/2}\right],$$

(*c*) whereas if the flag were perfectly flexible, $R_2 = 0$, the system is unstable at all length scales,

$$\omega = -k\frac{1 \pm i\left(\frac{R_1}{2}\right)^{1/2}|k|^{1/2}}{1 + \frac{1}{2}R_1|k|}.$$

(*d*) Hence, rigidity stabilizes while mass destabilizes. A critical condition for cross-over from stability to instability is predicted by asking when the fundamental mode, $k = 2\pi$, at the flag length becomes unstable. This occurs when $d_{2\pi} = 8\pi^3R_1R_2 + 4\pi^2R_2 - 2R_1 = 0$.

This condition was used by Shelley et al. (2005) to predict that there would be a critical flow speed U above which the SS state becomes unstable, as was also observed by Watanabe et al. (2002) [or equivalently, a critical length L as observed by Zhang et al. (2000)].

Alben (2008b) generalized this linearized model to encompass a finite-length flag coupled to a vortex sheet. The coupling of the temporal flapping to the spatial structure of the wake makes this a nonlinear eigenvalue problem. By solving this problem numerically, Alben showed, for example, that as the rigidity R_2 is reduced, an increasing number of high spatial-frequency modes become unstable, and there is a correlation between the number of unstable linear modes and the complexity of nonlinear dynamics (discussed below). Fitt & Pope (2001) earlier posed an approximate nonlocal model of a finite-length flag. Their model assumes small deflections, uses a quasi-steady version of Bernoulli's equation on the flag, and neglects the presence of a shed wake. They examined the effect of leading-edge boundary conditions and system parameters upon flag stability and predicted, for example, the existence of a critical flow velocity beyond which a flag becomes unstable. In a later, more elaborate treatment, Argentina & Mahadevan (2005) retained the effect of added mass, modeled the effect of vortex shedding from the trailing end, and avoided nonlocal calculation of a velocity potential by using an analytical approximation from slender

airfoil theory (Milne-Thompson 1960). Their analysis identifies a critical flow velocity beyond which the flag becomes unstable to flutter, and they interpret this transition as the excitation of a resonant bending instability. They ascribe some of the discrepancies of their theoretical predictions from the experimental measurements of Watanabe et al. (2002) to the lack of a viscously induced tension, which they subsequently model using Blasius boundary-layer theory. Manela & Howe (2009a) adapted this model to study the effect of boundary conditions (clamped versus free) at the head of the flag and investigated sound production by a flapping flag. Manela & Howe (2009b) further investigated the possible effects of a stream of shed vortices from an upstream flag pole. Finally, in addition to their experiments, Eloy et al. (2008) built upon earlier work and investigated a linear model that includes the effect of 3D nonlocal flows about a plate of finite span (see Eloy et al. 2007) that sheds circulation into the flow. This identifies critical velocities for transition to instability as a function of system parameters and shows better agreement with their data.

2.2.3. Nonlinear simulations. **Figure 3** shows numerical simulations from Alben & Shelley's (2008b) flag-fluid model. The underlying numerical methods are quite involved; X, $[p]$, and γ are expanded as first-kind Chebyshev polynomials to ease the evaluation of the finite nonlinear Hilbert transform over C_b in Equation 3. For stability, the system is discretized implicitly in time (to second order) and solved via Newton iteration at each time step. To control catastrophic ill-posedness of the free sheet (Moore 1979), the Birkhoff-Rott integral over C_f is regularized via Krasny (1986) regularization. Details on the numerical methods can be found in Alben (2009a).

These simulations recovered much of the phenomena observed in experiment. For fixed mass ratio R_1 **Figures 3*a–c*** show long-time dynamics of the flapping sheet, as the effective rigidity R_2 (or, equivalently, inverse velocity) is decreased. Each simulation showed an initial exponential

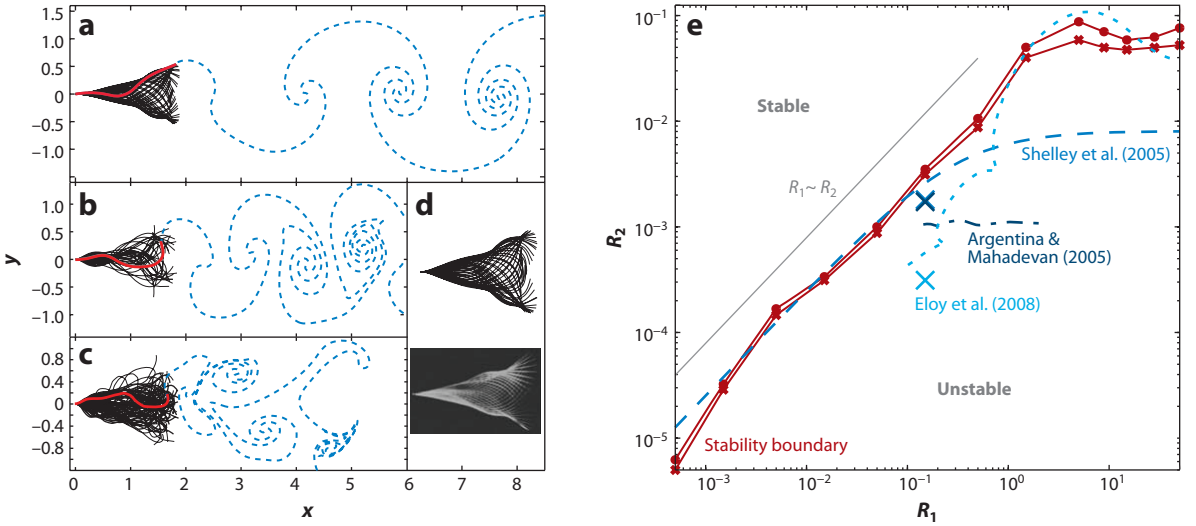

Figure 3

(*a–c*) Snapshots of flag simulations for fixed mass and decreasing rigidity. (*d*) A comparison of a model flag's flapping envelope with that reported by Watanabe et al. (2002). Panels *a–d* taken from Alben & Shelley (2008b). (*e*) The stability boundary (*solid line*) for the stretched-straight state in the R_1 R_2 plane, computed from simulations. Comparison is made with reduced models in the literature: Shelley et al. (2005) (*long-dashed line*); Argentina & Mahadevan (2005) (*dash-dotted line*); and Eloy et al. (2008) (*short-dashed line*). Panel *e* taken from Alben & Shelley (2008a).

growth away from being nearly flat, although if R_2 were sufficiently large, the initial perturbation would decay (shedding can move perturbations from the flag into the wake). At the larger R_2 (**Figure 3*a***), the flag shows a simple harmonic flapping, but as R_2 is decreased, the number of spatial and temporal degrees of freedom increases, sometimes abruptly. Associated with this increase is an increase in compression and complexity of the wake (**Figure 3*b***), and finally very irregular flapping and wake accompanied by a very broad-band spectral signature that one would associate with chaotic behavior (**Figure 3*c***; cf **Figure 2*d***). These simulations also show bistability of the SS and flapping states, although over a much smaller range than is observed in experiment, perhaps reflecting the lack of dissipative skin friction in the model. Finally, **Figure 3*e*** compares the stability boundary computed from the nonlinear simulations with those predicted by the recent approximate theories discussed above.

In a closely related approach, Michelin et al. (2008) have developed a simpler, but fully nonlinear, model wherein the continuous vortex sheet shed by the flexible flag is replaced by the shedding of discrete point vortices with unsteady strengths. With this method they recover, again, much of what is observed in experiment and by Alben & Shelley (2008b), such as various flapping states and the bistability of SS and flapping states.

2.2.4. Simulations with viscous effects. In the simulations of Alben & Shelley (2008b), the effects of viscosity—for example, by inducing drag—were captured through the shedding of a vortex sheet. Oddly, the numerical methods necessary for simulating such a classical model have only recently matured. The first simulations of flag-fluid interactions were of flexible sheets held in a fully viscous fluid described by the Navier-Stokes equations. For the first such simulation of which we are aware, Zhu & Peskin (2002) developed a new variant of the immersed boundary method (Mittal & Iaccarino 2005, Peskin 1981). Although the Reynolds number of the simulations was modest in comparison with experiment (2×10^2 versus 2×10^4), their simulations found that sustained flapping required that the flag have a certain minimum mass; that the SS state was stable regardless of mass if the flag were sufficiently short, but unstable to flapping at longer lengths; and that the SS and flapping states could show bistability. The mass of the flag was accounted for within the immersed boundary formulation by adding a singular immersed boundary density to the fluid density within the momentum balance equation. After appropriate regularization, the system is discretized in time using a fractional step pressure projection scheme, in which the nonuniformity in density yields a variable coefficient elliptic problem for the pressure correction. This is solved rather expensively using a multigrid iteration. This expense was partially addressed in subsequent work by Kim & Peskin (2008) in which the introduction of lagged tether points carrying mass circumvented the necessity of solving a variable coefficient elliptic problem, although at the cost of introducing a new small timescale into the problem. Although the problem of flag flapping is not addressed systematically, with this new method Kim & Peskin simulated the flapping of a finite 2D flag, at $Re = 340$, in a 3D fluid flow, together with the effects of the flag pole and the downward pull of gravity.

Using an adaptation of a commercial package wherein the flag is treated as an articulated pendulum under pressure loading, Farnell et al. (2004b) observed persistent flapping if the flag were sufficiently long. Yu (2005) extended the Lagrange-multiplier/fictious-domain methods of Glowinski et al. (1999), developed for fluid/rigid-body interactions, to interactions with flexible bodies. Yu applied these methods to the interaction of a flexible flag with the surrounding fluid flow (with $Re = 500$) and, like Zhu & Peskin (2002), recovered aspects of the experiments such as sustained flapping and bistability. Sawada & Hisada (2006) found similar results using an ALE finite-element method, as did Huang et al. (2007), who developed another version of the immersed boundary method to handle the mass of the flag.

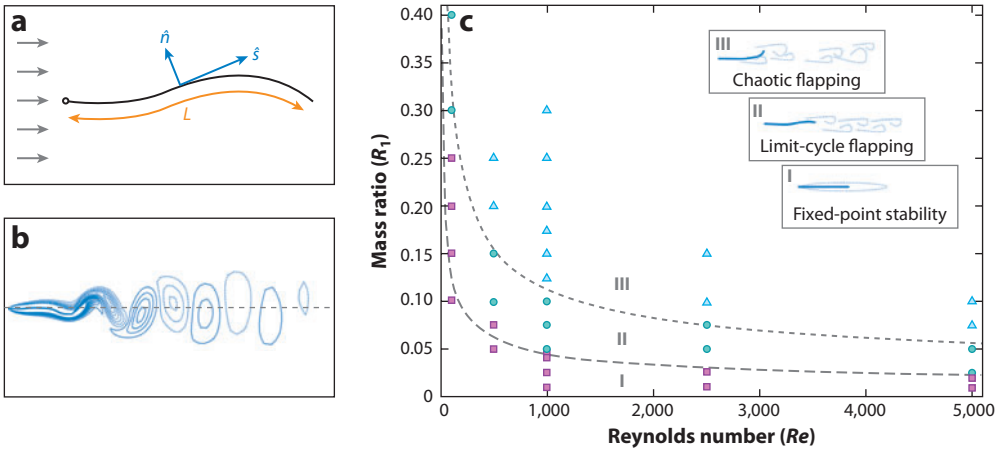

Figure 4

(*a*) A schematic of a flag held at its leading edge and flapping in an oncoming flow. (*b*) A sample simulation from Connell & Yue (2007), who used a numerical method based on body-fitted coordinates. (*c*) A phase diagram from Connell & Yue (2007), which for fixed rigidity R_2 shows the regimes of various flag-fluid states (stretched-straight, coherent, and chaotic) as a function of mass ratio R_1 and Reynolds number Re.

The most comprehensive of these fully viscous studies is due to Connell & Yue (2007). They developed a numerical scheme based on transforming the planar coordinates to body-conforming coordinates that move with the flexible surface. Finite differences are used in space, and time integration was accomplished via a second-order BDF scheme. Incompressibility was imposed by using the Chorin (1968) projection method. Code validation studies gave convergence somewhere between first and second order in space, and second order in time.

Figure 4*b* shows a sample simulation of a flag flapping at $Re = 1{,}000$. This is taken from a series wherein the flag rigidity R_2 is fixed and mass ratio R_1 is systematically increased (see Connell & Yue 2007, figure 9). This route through the parameter space gives qualitatively the same series of states observed in experiments (Watanabe et al. 2002, Zhang et al. 2000) and the vortex-sheet simulations (Alben & Shelley 2008b). At sufficiently small mass ratio R_1, the SS state is stable. Increasing R_1 leads to simple harmonic flapping with a narrow power spectrum (as for **Figure 4*b***). As R_1 is increased, the flapping dynamics becomes increasingly irregular, as does the wake, and the power spectrum broadens and is populated by multiple frequencies. A phase diagram of their results is shown in **Figure 4*c***.

Connell & Yue also identified the bistability of SS and flapping states, provided a descriptive analogy of the associated hysteresis of states in terms of the Duffing equation, and gave a somewhat phenomenological treatment of linear stability, which agrees well with their simulations.

3. VARIANTS ON THE FLAPPING PROBLEM

There have been several interesting variants studied of flag-fluid interactions, mostly having to do with the interactions of multiple bodies in various configurations. One example is given by Zhang et al. (2000), who studied the interactions of two proximal and parallel flags experimentally. The system is thus that of flow through an open compliant or collapsible tube (e.g., see Pedley & Lou 1998) whose walls are fixed at the inlet. Unsurprisingly, they observed that when the two walls were sufficiently far apart, the flags would flap asynchronously and independently. When brought

closer together, the dynamics transitioned to synchronized flapping with out-of-phase waves on the opposing flags. Each flapping period brings a bolus of fluid through the tube, fluxing it out the bottom. If the flags were brought together more closely, the flapping became in phase and gave a much more continuous flux of fluid through the system and a much different wake structure (see Zhang et al. 2000, figure 4).

The dynamics of two hydrodynamically coupled flags has been further studied both experimentally and theoretically. First again, Zhu & Peskin (2003) used their modified immersed boundary method to study this case, finding agreement with the experiments despite having a much smaller Reynolds number. Farnell et al. (2004a) have also numerically simulated this system and additionally analyzed the changing frequency content with filament separation, finding good agreement with experiment.

In a nice combined theory and experimental paper, Jia et al. (2007) reconstituted the soap-film experiments of Zhang et al. (2000) of two side-by-side filaments and compared their results with the predictions of the model of Shelley et al. (2005) (that is, Equations 6 and 7) generalized to include filament-filament hydrodynamic coupling, finding good qualitative agreement. Alben (2009b) also reproduced these findings using vortex-sheet models of hydrodynamically coupled flags and wakes, as in Alben & Shelley (2008b).

In seeking to understand the effect of body flexibility on drafting within moving aggregates of swimmers, Ristroph & Zhang (2008) studied drag on collections of flexible filaments whose leading edges were held fixed in an oncoming soap-film flow. For one filament trailing the other, they found that the leader, rather than the follower, could experience significant reduction in drag. The authors referred to this as inverted drafting (see **Figure 5**). This is contrary to the case of objects of (roughly) fixed shapes, such as race cars and bicyclists, where the trailing body experiences lower drag (see Jia & Yin 2008 for a similar study but with slightly different emphases). Subsequently, Zhu (2009) was able to reproduce these results in simulations using the immersed boundary method. Alben (2009b) also reproduced these results within the vortex-sheet formulation and equated the phenomenon of inverted drafting with constructive interactions of the two wakes of the tandem bodies creating strong trailing vortices.

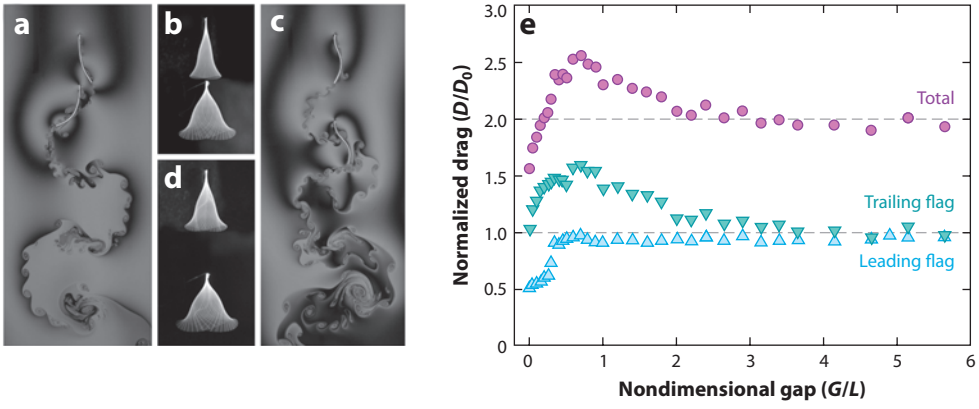

Figure 5

(*a*,*c*) The wake structure of two filaments, held in tandem at a fixed separation distance, as they flap in a flowing soap film. (*b*,*d*) The temporal dynamics and flapping amplitudes shown stroboscopically. (*e*) The time-averaged drag for the leading and trailing flags, both separately and together. Figure taken from Ristroph & Zhang (2008).

4. BENDING OF FLEXIBLE SHEETS BY FLOWS

The flapping instability of flags aligned with a flow is produced by the growth of traveling waves. A very different, but likewise interesting regime concerns the bending of elastic bodies that are instead obstructing a flow. Such a situation is part of the life of many sessile organisms such as trees (Niklas 1998) and seaweeds (Koehl 1996, Stewart 2006), whose morphologies are intimately related to the air and water fluid flows they must endure to survive. Indeed, the reconfiguration of flexible bodies by fluid flows is common in nature and can yield substantial and beneficial drag reduction (Denny 1994, Koehl 1984). A particularly elegant and clear example is provided by Vogel (1989), who studied the relation between drag and shape configuration of tree leaves in typical wind speeds. As wind speed increased, the leaves rolled themselves into ever tighter cones, a self-streamlining mediated by body flexibility that yielded a drag growth slower than the classical rigid-body U^2 law (see **Figure 6*a***). Garg & Husain (2003) reported a similar wind-driven reconfiguration in alpine flowers.

Our laboratory took this as a motivating example to study self-streamlining in a simpler setting (Alben et al. 2002, 2004). Using again a soap-film tunnel, we considered the bending of a flexible fiber (here a length of fiber-optic glass) mounted at its center and held transverse to the oncoming flow. This is a 1D leaf in a 2D wind. For low flow speeds, the filament remains nearly straight, and from its extended ends are shed sharp shear layers. The wake extends downstream, is roughly symmetric, and moves very slowly relative to the outer flow. As the flow speed increases, the fiber becomes more bent and streamlined. As a function of flow speed and other parameters, the drag on the fiber, the fiber shape, and wake structure were all recorded simultaneously, with Reynolds numbers ranging from 2,000 to 40,000. From these experiments and associated theory, we hoped

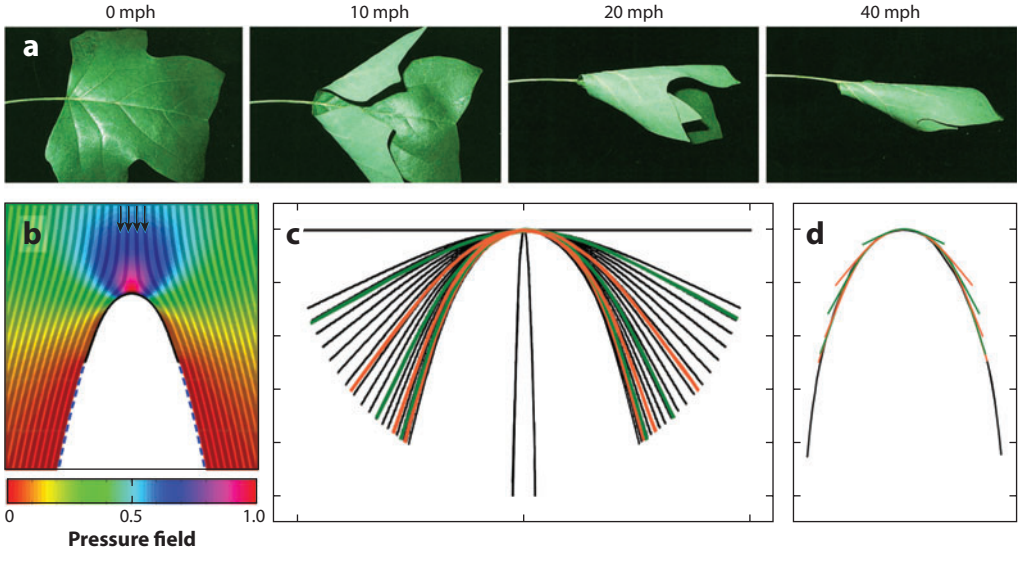

Figure 6

(*a*) The wind-driven reconfiguration of a broad tree leaf being held in a wind tunnel. Figure used with permission from S. Vogel. (*b*) A representative numerical solution of the free-streamline problem for flow around a flexible body. Shown are the body and dividing streamline, pressure field, and flow streamlines. Pressure field normalized to (0, 1). Figure taken from Alben et al. (2002). (*c*) The continuum of computed shapes as η is varied (*black curves*). Superimposed in alternating color are shapes taken from experiment. (*d*) The collapse of filament shapes onto a universal shape, by dilation of space with $\eta^{2/3}$.

to discover an exponent α that corrected the classical drag law to $U^{2-\alpha}$, and so accounted for velocity-dependent shape change.

Looking at steady-state behavior, we modeled this system using a generalization of free-streamline theory (Helmholtz 1868, Hureau et al. 1996) to construct simple steady flows around surfaces whose shapes were given by the balance of bending, tensile, and fluid pressure forces (that is, described by Equation 5 in the steady case). **Figure 6*b*** shows one computed case. After nondimensionalization, the system retains a single control parameter η, which is essentially $R_2^{-1/2}$ and so is the nondimensional flow velocity:

$$\eta = \left(\frac{\rho f L^3 U^2/2}{E} \right)^{1/2},$$

where f is the soap-film thickness. Furthermore, we note that η can be expressed as the ratio of filament length L to an intrinsic length L_0: $\eta = (L/L_0)^{3/2}$, where $L_0 = (2E/\rho f U^2)^{1/3}$. If this intrinsic length, which scales as $U^{-2/3}$, defines the effective cross section of the body to the flow, we then expect that at large velocities the fluid drag on this deformable body will scale as $U^{2-2/3} = U^{4/3}$, and hence $\alpha = 2/3$.

This is exactly the scaling behavior found in our numerical solutions of the nonlinear free-streamline problem and is consistent with our experimental results performed over three decades in η by varying U, L, and E. At small η we observe very slight bending of the beam and an η^2 scaling of the drag. Beyond some $\eta = O(1)$, the beam begins to bend more rapidly, and for large η a new scaling, $\eta^{4/3}$ for theory and presumably that for experiments, emerges for the drag. We found that in comparing experiment and theory, like shapes gave like drags (see **Figure 6*c***) and that the respective values of η for the corresponding theoretical and experimental shapes differed almost uniformly by a factor of 2.8. We interpreted this as the effect of unmodeled back pressure in the experiment's finite-sized wake. We found also that $L_0 = L\eta^{-2/3}$ set a length scale for self-similarity and that, by dilating space isotropically by $\eta^2/3$, both theoretical and experimental shapes collapsed onto a universal quasi-parabolic form, shown in **Figure 6*d***. In Alben et al. (2004) this universal streamlined shape, and the system's limiting drag characteristics, was constructed asymptotically.

Several numerical studies, using the immersed boundary method, followed from Zhu and his collaborators. These simulations account for the effects of viscosity, although at relatively low Reynolds numbers, and for time-dependent effects such as the susceptibility of the wake to Kelvin-Helmholtz and von Kármán instabilities. For Reynolds numbers in the $O(100)$ range, Zhu & Peskin (2007) reported significant drag reduction for a flexible fiber relative to a rigid fiber, a significant effect of bending rigidity upon drag, and a decreasing drag coefficient with increasing length of the fiber. Zhu (2007) presented a more in-depth study over a larger range in Reynolds number (up to 800), showing that, although the Reynolds number has a large effect on the shedding of vortices and fiber vibrations, it has little effect on time-averaged drag. Zhu also showed that fiber length and rigidity were important determinants in vortex shedding and fiber vibration. Finally, Zhu (2008) provided numerical evidence that the power law of drag with flow velocity decreases from 2 toward 4/3 as Reynolds number is increased.

The above results were all for a 2D model problem. Schouveiler & Boudaoud (2006) revisited the original motivating problem of Vogel (1989) and presented a combined experimental and theoretical study of the rolling up of sheets into cones in a 3D uniform flow. To do this, they cut circular sheets from edge to center, allowing them to bend into a cone when in a wind, and measured the drag and cone angle as a function of wind speed. They found that the wind-driven reconfiguration yielded a decrease in drag coefficient with wind speed. An approximate potential

flow model was constructed, and they could collapse their data when plotted against a so-called elastohydrodynamical number, which is essentially R_2 with a logarithmic correction arising from a cutoff in cone radius at its tip. They also predicted the same drag scaling as in Alben et al. (2002), although a different scaling for shape.

Finally, in very recent work Gosselin et al. (2010) studied experimentally the reconfiguration of flexible structures—flat plates and overlapping plates arranged to form a disk—by a steady air flow, as well as reanalyzed the experimental results of Alben et al. (2002, 2004) from soap-film flows. They showed, for example, that both wind-tunnel and soap-film data can be collapsed together when nondimensional drag and squared speed η^2 are scaled appropriately by a partly empirical drag coefficient. They also showed that their collapsed data for both plates and disks, as well as the reconfigured body shapes, can be well fit by a simple nonlinear theory that balances bending forces against a squared drag relation that accounts for the local inclination of the body to the oncoming flow and that contains two experimentally determined coefficients.

5. OUTLOOK

The combination of detailed experiment, sophisticated modeling, and increasingly accurate numerical simulation has much improved our understanding of archetype problems in fluid-flexible body interactions and will have a profound impact on our ability to understand more complex situations. Still, most of theoretical analyses have been posed in two dimensions, and moving these, particularly those based on numerical simulation, to three dimensions remains a challenge. Another theoretical and experimental challenge is to understand the robustness of various dynamical flapping states to the external flow disturbances found in natural settings. And although the work of Connell & Yue (2007) gives a first step toward an analytical understanding of hysteresis and bistability of SS and flapping states, we still lack a first-principles model system that can be directly studied.

As implied above, there remains the task of embedding our understanding of these relatively stripped-down systems into more difficult flow-structure problems. This is relevant to applications such as energy harvesting by flow-induced oscillations of flexible structures (Allen & Smits 2001), or to asking how flexibility impedes or assists propulsive motions of organisms or devices. There is a developing body of work beginning to address just these kinds of questions (e.g., see Alben 2008a, Liao et al. 2003, and Michelin & Llewellyn-Smith 2009 for studies related to this review). Indeed, much of the research discussed here sheds light on, or is inspired by, problems in biological locomotion in which animals exploit a mix of active and passive responses to move efficiently. Understanding how passive responses—whether built into structure geometry, or in material and fluidic behaviors—are exploited has been a central theme of our own laboratory (e.g., Alben & Shelley 2005, Childress et al. 2006, Vandenberghe et al. 2004).

DISCLOSURE STATEMENT

The authors are not aware of any affiliations, memberships, funding, or financial holdings that might be perceived as affecting the objectivity of this review.

ACKNOWLEDGMENTS

We would like to thank our colleagues S. Childress and C. Peskin for many helpful conversations on topics related and unrelated to this review and S. Alben and L. Zhu for their continued scientific

collaborations with our lab. We also thank the Department of Energy and the National Science Foundation for their support.

LITERATURE CITED

Alben S. 2008a. Optimal flexibility of a flapping appendage in an inviscid fluid. *J. Fluid Mech.* 614:355–80

Alben S. 2008b. The flapping-flag instability as a nonlinear eigenvalue problem. *Phys. Fluids* 20:104106

Alben S. 2009a. Simulating the dynamics of flexible bodies and vortex sheets. *J. Comput. Phys.* 228:2587–603

Alben S. 2009b. Wake-mediated synchronization and drafting in coupled flags. *J. Fluid Mech.* 641:489–96

Alben S, Shelley M. 2005. Coherent locomotion as an attracting state for a free flapping body. *Proc. Natl. Acad. Sci. USA* 102:11163–66

Alben S, Shelley M. 2008a. Erratum: Flapping states of a flag in an inviscid fluid: bistability and the transition to chaos. *Phys. Rev. Lett.* 101:119902

Alben S, Shelley M. 2008b. Flapping states of a flag in an inviscid fluid: bistability and the transition to chaos. *Phys. Rev. Lett.* 100:074301

Alben S, Shelley M, Zhang J. 2002. Drag reduction through self-similar bending of a flexible body. *Nature* 420:479–81

Alben S, Shelley M, Zhang J. 2004. How flexibility induces streamlining in a two-dimensional flow. *Phys. Fluids* 16:1694–713

Allen J, Smits A. 2001. Energy harvesting eel. *J. Fluids Struct.* 15:629–40

Argentina M, Mahadevan L. 2005. Fluid-flow-induced flutter of a flag. *Proc. Natl. Acad. Sci. USA* 102:1829–34

Bisplinghoff R, Ashley H. 2002. *Principles of Aeroelasticity*. New York: Dover

Carrier G, Krook M, Pearson C. 1966. *Functions of a Complex Variable: Theory and Technique*. New York: McGraw-Hill

Childress S, Vandenberghe N, Zhang J. 2006. Hovering of a passive body in an oscillating airflow. *Phys. Fluids* 18:117103

Chorin A. 1968. Numerical solution of the Navier-Stokes equations. *Math. Comput.* 22:745–62

Connell B, Yue D. 2007. Flapping dynamics of a flag in a uniform stream. *J. Fluid Mech.* 581:33–68

Couder Y, Chomaz JM, Rabaud M. 1989. On the hydrodynamics of soap films. *Physica D* 37:384–405

Crighton D, Oswell J. 1991. Fluid loading with mean flow 0.1. Response of an elastic plate to localized excitation. *Philos. Trans. R. Soc. Lond. Ser. A* 335:557–92

de Langre E, Paidoussis M, Doare O, Modarres-Sadeghi Y. 2007. Flutter of long flexible cylinders in axial flow. *J. Fluid Mech.* 571:371–89

Denny M. 1994. Extreme drag forces and the survival of wind-swept and water-swept organisms. *J. Exp. Biol.* 194:97–115

Eloy C, Lagrange R, Souilliez C, Schouveiler L. 2008. Aeroelastic instability of cantilevered flexible plates in uniform flow. *J. Fluid Mech.* 611:97–106

Eloy C, Souilliez C, Schouveiler L. 2007. Flutter of a rectangular plate. *J. Fluids Struct.* 23:904–19

Farnell D, David T, Barton D. 2004a. Coupled states of flapping flags. *J. Fluids Struct.* 19:29–36

Farnell D, David T, Barton D. 2004b. Numerical simulations of a filament in a flowing soap film. *Int. J. Numer. Methods Fluids* 44:313–30

Fitt A, Pope M. 2001. The unsteady motion of two-dimensional flags with bending stiffness. *J. Eng. Math.* 40:227–48

Garg A, Husain T. 2003. Strategies adopted by the alpine genus *Pedicularis* L. (Scrophulariaceae) to overcome environmental stress. *Curr. Sci.* 85:1413–14

Gharib M, Derango P. 1989. A liquid-film (soap film) tunnel to study two-dimensional laminar and turbulent shear flows. *Physica D* 37:406–16

Glowinski R, Pan TW, Hesla T, Joseph D. 1999. A distributed Lagrange multiplier/fictitious domain method for particulate flows. *Int. J. Multiphase Flow* 25:755–94

Gosselin F, De Langre E, Machado-Almeida B. 2010. Drag reduction of flexible plates by reconfiguration. *J. Fluid Mech.* 650:319–41

Helmholtz H. 1868. Uber discontinuierliche flussigkeitsbewegungen. *Monatsber. Berlin Akad.* 23:215–68

Huang W, Shin S, Sung S. 2007. Simulation of flexible filaments in a uniform flow by the immersed boundary method. *J. Comp. Phys.* 226:2206–28
Huber G. 2000. Swimming in Flatsea. *Nature* 408:777–78
Hureau J, Brunon E, Legallais P. 1996. Ideal free streamline flow over a curved obstacle. *J. Comput. Appl. Math.* 72:193–214
Jia L, Li F, Yin X, Yin X. 2007. Coupling modes between two flapping filaments. *J. Fluid Mech.* 581:199–220
Jia L, Yin X. 2008. Passive oscillations of two tandem flexible filaments in a flowing soap film. *Phys. Rev. Lett.* 100:228104
Jones M. 2003. The separated flow of an inviscid fluid around a moving flat plate. *J. Fluid Mech.* 496:405–41
Jones M, Shelley M. 2005. Falling cards. *J. Fluid Mech.* 540:393–425
Kim Y, Peskin C. 2008. Penalty immersed boundary method for an elastic boundary with mass. *Phys. Fluids* 19:053103
Koehl M. 1984. How do benthic organisms withstand moving water. *Am. Zool.* 24:57–70
Koehl M. 1996. When does morphology matter? *Annu. Rev. Ecol. Syst.* 27:501–42
Krasny R. 1986. Desingularization of periodic vortex sheet roll-up. *J. Comput. Phys.* 65:292–313
Liao JC, Beal DN, Lauder GV, Triantafyllou MS. 2003. Fish exploiting vortices decrease muscle activity. *Science* 302:1566–69
Manela A, Howe MS. 2009a. On the stability and sound of an unforced flag. *J. Sound Vibr.* 321:994–1006
Manela A, Howe MS. 2009b. The forced motion of a flag. *J. Fluid Mech.* 635:439–54
Michelin S, Llewellyn-Smith S. 2009. Resonance and propulsion performance of a heaving flexible wing. *Phys. Fluids* 21:071902
Michelin S, Llewellyn-Smith S, Glover B. 2008. Vortex shedding model of a flapping flag. *J. Fluid Mech.* 617:1–10
Milne-Thompson L. 1960. *Theoretical Hydrodynamics*. New York: Macmillan
Mittal R, Iaccarino G. 2005. Immersed boundary methods. *Annu. Rev. Fluid Mech.* 37:239–61
Moore D. 1979. Spontaneous appearance of a singularity in the shape of an evolving vortex sheet. *Proc. R. Soc. A* 365:105–19
Muller U. 2003. Fish 'n flag. *Science* 302:1511–12
Niklas K. 1998. The influence of gravity and wind on land plant evolution. *Rev. Paleobot. Palynol.* 102:1–14
Paidoussis M. 2004. *Fluid-Structure Interactions: Slender Structures and Axial Flow*, Vol. 2. London: Elsevier
Pedley T, Lou X. 1998. Modelling flow and oscillations in collapsible tubes. *Theor. Comput. Fluid Dyn.* 10:277–94
Peskin C. 1981. The fluid dynamics of heart valves: experimental, theoretical and computational methods. *Annu. Rev. Fluid Mech.* 14:235–59
Rayleigh L. 1879. On the instability of jets. *Proc. Lond. Math. Soc.* 10:4–13
Ristroph L, Zhang J. 2008. Anomalous hydrodynamical drafting of interacting flapping flags. *Phys. Rev. Lett.* 101:194502
Rutgers M, Wu X, Daniel W. 2001. Conducting fluid dynamics experiments with vertically falling soap films. *Rev. Sci. Instrum.* 72:3025–37
Saffman P, Baker G. 1979. Vortex interactions. *Annu. Rev. Fluid Mech.* 11:95–121
Sawada T, Hisada T. 2006. Fluid-structure interaction analysis of a two-dimensional flag-in-wind problem by the ALE finite element method. *JSME Int. J. Ser. A* 36:170–79
Schouveiler L, Boudaoud A. 2006. The rolling up of sheets in a steady flow. *J. Fluid Mech.* 563:71–80
Shelley M, Vandenberghe N, Zhang J. 2005. Heavy flags undergo spontaneous oscillations in flowing water. *Phys. Rev. Lett.* 94:094302
Shen L, Zhang X, Yue D, Triantafyllou M. 2003. Turbulent flow over a flexible wall undergoing a streamwise traveling wave motion. *J. Fluid Mech.* 484:197–221
Stewart H. 2006. Hydrodynamic consequences of flexural stiffness and buoyancy for seaweeds: a study using physical models. *J. Exp. Biol.* 209:2170–81
Taneda S. 1968. Waving motions of flags. *J. Phys. Soc. Jpn.* 24:392–401
Vandenberghe N, Zhang J, Childress S. 2004. Symmetry breaking leads to forward flapping flight. *J. Fluid Mech.* 506:147–55

Vogel S. 1989. Drag and reconfiguration of broad leaves in high winds. *J. Exp. Bot.* 40:941–48
Vogel S. 1994. *Life in Moving Fluids*. Princeton, NJ: Princeton Univ. Press. 2nd ed.
Watanabe Y, Suzuki S, Sugihara M, Sueoka Y. 2002. An experimental study of paper flutter. *J. Fluids Struct.* 16:529–42
Yu Z. 2005. A DLM/FD method for fluid/flexible-body interactions. *J. Comput. Phys.* 207:1–27
Zhang J, Childress S, Libchaber A, Shelley M. 2000. Flexible filaments in a flowing soap film as a model for one-dimensional flags in a two-dimensional wind. *Nature* 408:835–39
Zhu L. 2007. Viscous flow past a flexible fiber tethered at its center point: vortex shedding. *J. Fluid Mech.* 587:217–34
Zhu L. 2008. Scaling laws for drag of a compliant body in an incompressible viscous flow. *J. Fluid Mech.* 607:387–400
Zhu L. 2009. Interaction of two tandem deformable bodies in a viscous incompressible flow. *J. Fluid Mech.* 635:455–75
Zhu L, Peskin C. 2003. Interaction of two flapping filaments in a flowing soap film. *Phys. Fluids* 15:1954–60
Zhu L, Peskin C. 2007. Drag of a flexible fiber in a 2D moving viscous fluid. *Comp. Fluids* 36:398–406
Zhu LD, Peskin C. 2002. Simulation of a flapping flexible filament in a flowing soap film by the immersed boundary method. *J. Comput. Phys.* 179:452–68

Annual Review of
Fluid Mechanics

Volume 43, 2011

Contents

Indexes

Errata

An online log of corrections to *Annual Review of Fluid Mechanics* articles may be found at http://fluid.annualreviews.org/errata.shtml